

Single-Molecule Charge Transfer and Bonding at an Organic/Inorganic Interface: Tetracyanoethylene on Noble Metals

Daniel Wegner,^{*,†} Ryan Yamachika,[†] Yayu Wang,[†] Victor W. Brar,[†]
Bart M. Bartlett,[‡] Jeffrey R. Long,[‡] and Michael F. Crommie^{*,†}

*Department of Physics, University of California, Berkeley, Berkeley, and
Materials Sciences Division, Lawrence Berkeley National Laboratory,
Berkeley, California 94720-7300, and Department of Chemistry,
University of California, Berkeley, Berkeley, California 94720-1460*

Received August 31, 2007; Revised Manuscript Received November 2, 2007

ABSTRACT

We have studied the structural and electronic properties of tetracyanoethylene (TCNE) molecules on different noble-metal surfaces using scanning tunneling spectroscopy and density functional theory. Striking differences are observed in the TCNE behavior on Au, Ag, and Cu substrates in the submonolayer limit. We explain our findings by a combination of charge-transfer and lattice-matching properties for TCNE across substrates that results in a strong variation of molecule–molecule and molecule–substrate interactions. These results have significant implications for future organic/inorganic nanoscopic devices incorporating molecule-based magnetism.

Tetracyanoethylene (TCNE) is a strong electron acceptor with a large electron affinity¹ that readily forms charge-transfer complexes in which it pulls electrons from neighboring metal atoms or molecules.^{2,3} Within the rapidly developing field of molecule-based magnetism, charge-transfer compounds of the type M(TCNE)_x, where M is a paramagnetic transition-metal ion, form an important group of ferromagnets with potential applications due to their high Curie temperatures (up to ~400 K).^{4–7} Despite extensive studies, however, the origin of magnetic coupling in the TCNE-based compounds is not well understood.^{8–10} One of the major drawbacks is the lack of sufficient structural characterization, largely attributed to disordered growth: the higher T_C materials exhibit a lack of long-range periodicity. Since many potential applications involve ultrathin film and nanoscale cluster growth of molecule-based magnetic composites,¹¹ it is important to understand the microscopic structural and electronic properties of this molecule as it contacts different metallic substrates. So far the knowledge of TCNE adsorption on metallic substrates is quite sparse.^{12–14}

In order to clarify the properties of this molecular building block at organic/inorganic interfaces, we have performed

single-molecule scanning tunneling microscopy (STM) and spectroscopy (STS) measurements of TCNE on three different noble-metal surfaces: Au(111), Ag(100), and Cu(100). We observe increasingly strong molecule–substrate binding as we move from Au to Ag to Cu, and the molecular growth patterns on these noble-metal surfaces are all strikingly different. On Au(111), the TCNE molecules tilt onto their sides and form loosely bound islands, whereas TCNE molecules on Ag(100) lie flat and prefer to remain as isolated monomers. TCNE on Cu(100), on the other hand, forms tightly bound compact island structures. This behavior can be explained by a combination of charge-transfer and lattice-matching properties for these different substrates that leads to differing degrees of intermolecular versus molecule–substrate interaction. Using density functional theory (DFT) calculations, we deduce that the behavior of TCNE on Au(111) is dominated by intermolecular quadrupole interactions, whereas TCNE behavior on Ag(100) is mainly influenced by charge-transfer-induced Coulomb interactions. TCNE behavior on Cu(100) appears to be dominated by strong chemical bonding between underlying Cu atoms and molecular cyano groups.

The experiments were performed in ultrahigh vacuum (UHV) using a home-built STM operated at $T = 7$ K. Single-crystal substrates of Au(111), Ag(100), and Cu(100) were cleaned prior to molecule deposition by standard sputter-

* To whom correspondence should be addressed. E-mail: wegner@berkeley.edu; crommie@berkeley.edu.

[†] Department of Physics, University of California, Berkeley and Lawrence Berkeley National Laboratory.

[‡] Department of Chemistry, University of California, Berkeley.

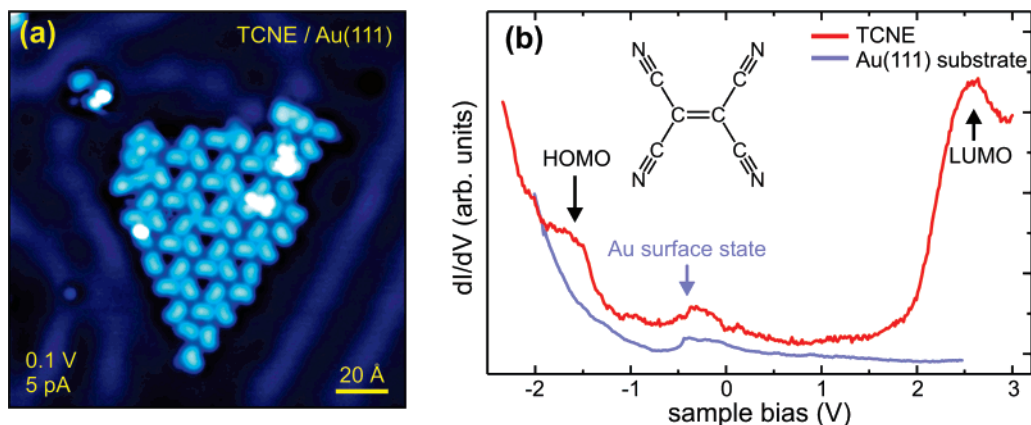


Figure 1. STM results of TCNE adsorption on Au(111). (a) TCNE molecules order in a loose hexagonal pattern within the fcc domains of the Au(111) herringbone reconstruction. (b) STS of TCNE/Au(111) shows a HOMO resonance at -1.5 eV and a LUMO resonance at $+2.5$ eV. The additional feature at about -0.5 eV is from the Au(111) surface state.

annealing procedures. TCNE crystals with 99% purity were kept in a small vacuum container and cleaned by repeated cycles of pumping and flushing with Ar gas before in situ deposition onto the noble-metal substrates at room temperature through a leak valve. The purity of the TCNE vapor was checked by quadrupole mass spectrometry. After deposition, the sample was transferred in situ to the cryogenic STM. Topography images were taken in constant-current mode, and STS was performed by measuring the differential conductance dI/dV as a function of the sample bias V by standard lock-in techniques (modulation 1–10 mV (rms), frequency ~ 451 Hz) under open-feedback conditions.

We begin by describing the behavior of TCNE deposited on Au(111). Figure 1a shows that TCNE adsorbates form open, loosely ordered islands within the larger face-centered cubic (fcc) domains of the Au-herringbone reconstruction. Each molecule appears as an elongated protrusion in the STM topography (~ 6 Å \times 9 Å) with an apparent height of ~ 1.2 Å and a slight kidney-like shape. Tunneling spectroscopy of TCNE/Au(111) (Figure 1b) shows peaks at -1.5 and $+2.5$ V relative to the Fermi energy ($V = 0 \equiv E_F$), which we assign to the highest occupied molecular orbital (HOMO) and lowest unoccupied molecular orbital (LUMO) states, respectively. Within this 4 eV wide gap, a spectral feature of the Au(111) surface state is visible at ~ -0.5 V.¹⁵ dI/dV maps of TCNE at the HOMO/LUMO energies show no significant energy dependence to the molecular appearance. TCNE molecules on Au(111) are easily manipulated by the STM tip via the sliding technique^{16,17} (typical manipulation parameters: 50 mV, 3 nA) and frequently jump to the tip during this process, indicating that TCNE is only weakly bound to Au(111).

TCNE shows very different adsorption behavior on Ag(100), as can be seen in Figure 2a. Molecules on this surface are found in isolated form on the Ag(100) terraces. In the topography each molecule appears as an oval protrusion (~ 6 Å \times 7 Å) surrounded by a dark ring (~ 12 Å in diameter) that dips deeply along the short axis of the oval. STM images with atomic substrate resolution indicate that TCNE adsorbs in two possible orientations (differing by 90°) with the molecular center (i.e., the C=C bond) on top of a

Ag atom. At low coverage the molecules remain isolated and do not assemble into islands on terraces (some limited island formation is observed at higher coverages $>10\%$ of a monolayer). STS performed on single TCNE/Ag(100) adsorbates reveals a broad HOMO state at -0.6 eV (Figure 2b). No other peaks are observed between -1.5 and $+2.5$ eV relative to E_F . dI/dV mapping of individual TCNE molecules at the HOMO energy reveals many single-molecule features not apparent in STM topography images: whereas the STM topograph (Figure 2c) is a broad oval, the HOMO dI/dV map (Figure 2d) shows a bright, elongated body that is intersected by a central line node and surrounded by four “legs”. Molecular manipulation (sliding) of TCNE/Ag(100) requires a closer tip–surface interaction than TCNE/Au(111) (typical TCNE/Ag(100) sliding parameters are 5 mV, 1–2 nA) and the molecules do not readily leave the surface, suggesting a stronger molecule–substrate interaction for TCNE/Ag(100) than for TCNE/Au(111).

TCNE deposited onto Cu(100) behaves completely different from either TCNE/Au or TCNE/Ag. As seen in Figure 3, TCNE molecules on Cu(100) order in straight chains along the $[110]$ and $[-110]$ directions with an intermolecular distance of ~ 8 Å. Neighboring chains create a square lattice where each TCNE molecule has an apparent height of ~ 0.6 Å. STS on TCNE/Cu(100) does not show any molecular resonances within ± 2 eV around E_F . Furthermore, we are completely unable to manipulate TCNE/Cu(100) adsorbates with the STM tip. Close-up STM topography reveals an intramolecular shape within TCNE/Cu(100) islands consisting of four “short legs” surrounding a bright elongated center (Figure 3b). Additional protrusions (i.e., “extended legs”) are visible at the borders of islands and chains (Figure 3b,c). The extended legs do not always appear, however (Figure 3c), and so we conclude that they are not a part of the intrinsic electronic structure of TCNE on Cu(100).

In order to understand the TCNE images that we observed on different noble-metal surfaces, we performed ab initio pseudopotential DFT calculations of isolated neutral and negatively charged TCNE molecules (TCNE⁰, TCNE⁻, and TCNE²⁻) using the SIESTA code with a double- ζ basis set

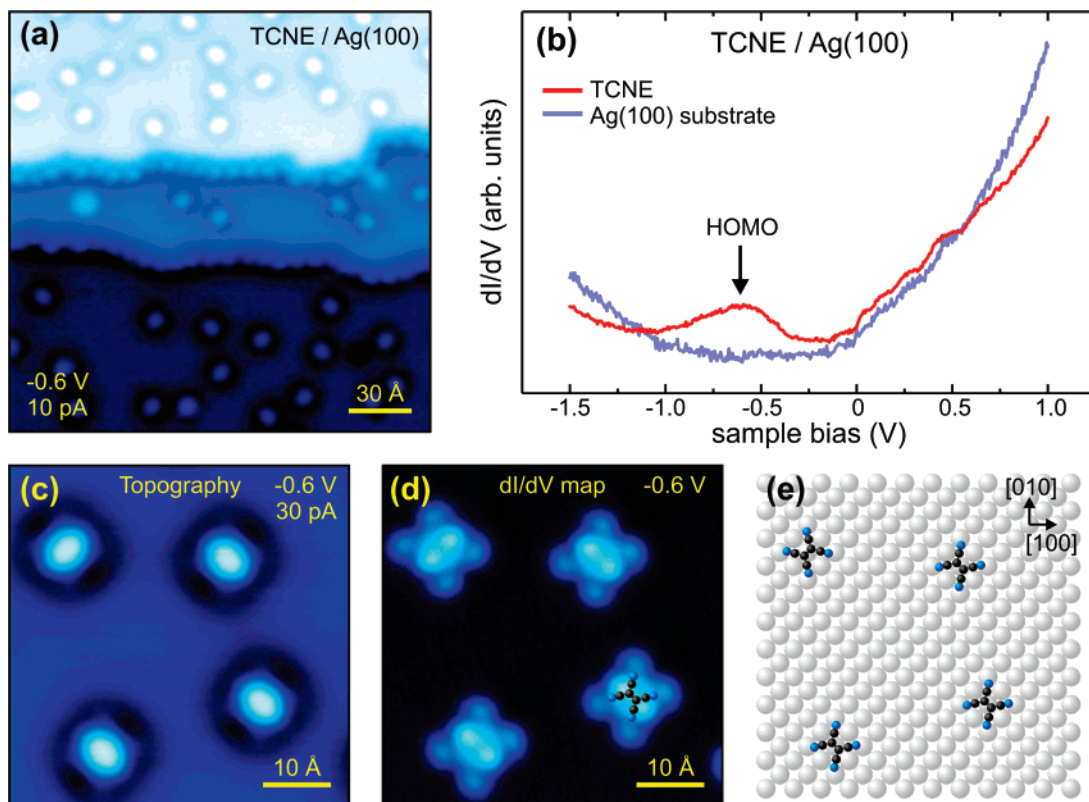


Figure 2. STM results of TCNE adsorption on Ag(100). (a) TCNE molecules on Ag(100) terraces adsorb as isolated molecules. (b) STS on isolated TCNE/Ag(100) molecules reveals a HOMO peak at -0.6 eV. (c) STM topograph and (d) simultaneously measured dI/dV map of four TCNE molecules on a Ag(100) terrace at the HOMO energy. (e) Structural model for TCNE/Ag(100) configuration seen experimentally in (c) and (d).

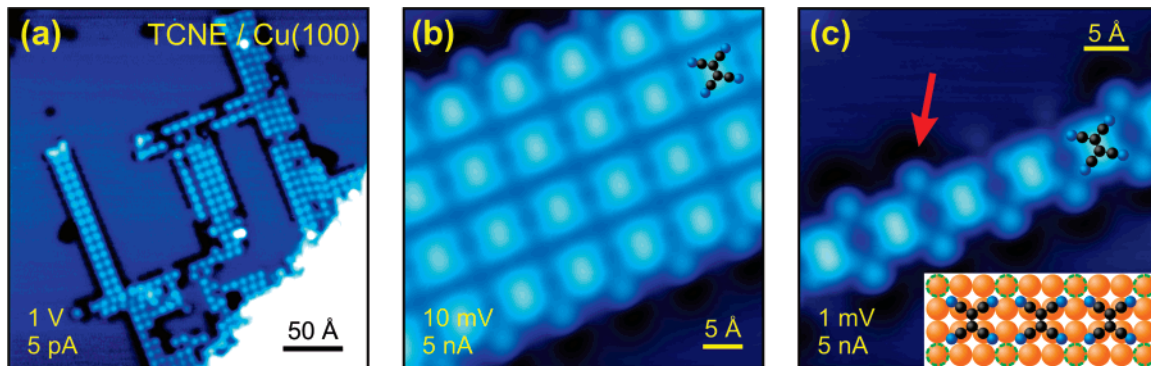


Figure 3. STM results of TCNE adsorption on Cu(100). (a) TCNE molecules order in long chains and islands with square symmetry. (b) Close-up images show that each TCNE/Cu(100) molecule has four “short legs” in compact arrangement. (c) Further protrusions (red arrow) can be seen at TCNE island edges due to a reconstruction (i.e., buckling) of the Cu-substrate atoms, indicating the formation of a metal-organic coordination network. Inset: proposed TCNE/Cu(100) structural model shows buckled Cu atoms outlined in green.

and the local density approximation.^{18,19} Theoretical LDOS isosurfaces of TCNE in the planar view look nothing like the kidney-shaped molecules experimentally observed for TCNE on Au(111). This provides evidence that TCNE/Au is likely not oriented with its molecular plane parallel to the Au(111) surface plane, and thus, in this case, we are likely experimentally imaging the “side view” of the orbital where just two cyano groups are dominant.

The situation is quite different for TCNE/Ag(100). Figure 4 compares the calculated HOMO isosurfaces of TCNE⁰ and TCNE²⁻ with the experimental HOMO dI/dV map of TCNE/Ag(100). (The calculated singly occupied molecular orbital

(SOMO) isosurface of TCNE⁻ and the LUMO of TCNE⁰ were all found to be structurally identical to the HOMO of TCNE²⁻.) Although the HOMO of TCNE⁰ shows an antinode in the molecule center, the HOMO isosurface of TCNE²⁻ shows pronounced nodes across the central C=C bond and the four C≡N triple bonds. The overall shape of the theoretical TCNE²⁻ HOMO isosurface is in very good agreement with the experimental dI/dV map of the HOMO state of TCNE/Ag(100) imaged at -0.6 V (Figure 4c). Therefore, we conclude that TCNE is negatively charged (i.e., either TCNE⁻ or TCNE²⁻) on Ag(100) due to charge transfer from the substrate. From the DFT results in Figure

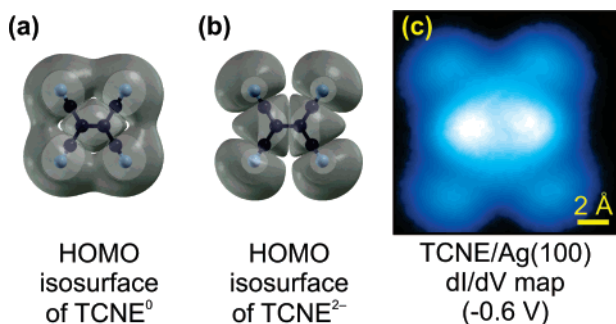


Figure 4. DFT calculations and comparison with experiments. (a) The DFT-calculated HOMO isosurface of isolated TCNE⁰ shows an antinode at the molecular center. (b) The calculated HOMO isosurface of an isolated TCNE²⁻ molecule displays a line node across the central C=C bond. (c) Experimental dI/dV map of TCNE/Ag(100) at HOMO energy closely resembles the calculated isosurface in (b).

4, we can also confirm the orientation of TCNE on Ag(100), as drawn in the structural model of Figure 2e.

We can understand the experimental TCNE/Cu(100) images if we assume that the four short legs within the interior of a TCNE/Cu island are the cyano groups of the molecules. In this case, the C=C double bond is oriented perpendicular to the chain-growth direction, as shown in the structural model inset to Figure 3c. An important difference between TCNE on Cu(100) and TCNE on Ag(100) is that the “extended legs” seen on the edges of TCNE/Cu(100) islands (Figure 3c) only occur sporadically even though they are robust topographic features. This is different from the TCNE/Ag(100) case, where extended legs are never visible in topographs but always appear in dI/dV maps. Combining this with the fact that TCNE cannot be manipulated on Cu(100) we conclude that the extended legs in the TCNE/Cu(100) case likely arise from strong chemical reaction between TCNE and Cu(100), resulting in a buckling of the Cu(100) surface atoms (buckled atoms are outlined with dashed green circles in the structural model in Figure 3c).

These strikingly different behaviors for TCNE on different noble-metal substrates are a consequence of the competition between molecule–molecule and molecule–substrate interactions. These interactions can be better understood by an electrostatic analysis of the different cases via comparison of electron affinities (EA).²⁰ Atomic Au has the largest EA, 2.31 eV,²¹ of the three substrates and therefore is less likely to establish a strong charge-transfer bond by donating electrons to the TCNE molecules (EA = 3.17 eV).¹ In this case, intermolecular interaction dominates TCNE behavior and TCNE cyano groups are not tightly bound to the Au substrate, leading to the observed out-of-plane ordering. The complex pattern seen for TCNE/Au(111) suggests that neighboring TCNE molecules are coupled through quadrupole interaction: the electronegative cyano groups point toward the electropositive center of the C=C bond of neighboring molecules, thus maximizing quadrupolar interaction for an out-of-plane geometry. Such tilted arrangements have also been seen in bulk pure TCNE crystals,^{22–24} and quadrupolar interaction is also known to play a role in the

submonolayer ordering of the closely related molecule TCNQ on Cu(111).²⁵

Because Ag has a much smaller EA of 1.30 eV,²¹ it is more likely to donate electrons to TCNE and increase molecule–substrate interaction (consistent with DFT results that imply a TCNE/Ag charge state of TCNE⁻ or TCNE²⁻). A weak charge-transfer bond is thus formed between TCNE and the substrate, inducing the molecule to bind in planar fashion. The negatively charged TCNE ions repel each other electrostatically, hindering closed-packed submonolayer growth as observed experimentally.

The EA of Cu (1.24 eV) differs only slightly from that of Ag,²¹ and so a consideration of EA alone does not adequately explain why TCNE adsorbs so differently on Cu(100) (self-assembling into chains and narrow islands) compared to the isolated molecules on Ag(100). A key difference between the Cu and Ag substrates, however, is their lattice constant. The nearest-neighbor interatomic distance is significantly smaller for Cu(100) (2.55 Å) than for Ag(100) (2.89 Å). In the TCNE/Cu(100) structural model shown in Figure 3c the lateral distance between the reactive nitrogen atoms of TCNE and the buckled Cu atoms is 2.37 Å, similar to the typical nitrogen–metal distance observed for charge-transfer complexes of TCNE with transition metals.^{9,26–28} During the initial growth of TCNE on Cu(100), the molecules diffuse on the metal terraces until they hit a step edge where the nitriles can easily connect to Cu atoms of the upper terrace. Substrate-mediated self-assembly of TCNE/Cu subsequently arises from the buckling of Cu surface atoms underneath the TCNE. This forms a potential well that traps other TCNE molecules since the buckled Cu atoms are likely to be positively charged due to electron transfer to the TCNE.^{25,27–29} The tendency of TCNE on Cu(100) to form chains rather than isotropic islands is a consequence of the resulting anisotropic electrostatic potential energy surface of TCNE in conjunction with the strong molecule–substrate interaction.³⁰ This also explains why the interaction of TCNE with the Ag(100) substrate is so much weaker than with the Cu(100) substrate. If one were to imagine the same structure for TCNE on Ag(100) as seen for TCNE on Cu(100), then the N–Ag distance would be 3.13 Å. This is outside the range of a typical charge-transfer bond, leading to a weaker interaction between TCNE and the Ag substrate and thus no substrate buckling. Electrostatic repulsion between the negatively charged TCNE molecules is therefore able to prevent self-assembly on Ag(100), unlike the case for Cu(100).

These results allow us to predict the structure of TCNE on other noble-metal surfaces. For example, we expect a rectangular self-assembly of TCNE on Au(100) that is dominated by intermolecular quadrupole interaction and exhibits a molecular plane perpendicular to the surface. In contrast, TCNE on Cu(111) will most likely grow in disordered fashion because the strong molecule–substrate interaction will tend to pin the molecules flat to the surface while a mismatch of lattice and molecular symmetries will prevent ordered self-assembly. Such assumptions are supported by observations of different charge states of TCNE

(ranging from TCNE⁰ up to TCNE³⁻) that occur simultaneously for TCNE/Cu(111).¹³

In summary, we have studied the adsorption of submonolayer amounts of TCNE on noble-metal surfaces via cryogenic STS. The exceptional differences in electronic and structural behavior observed on these surfaces is a consequence of different ratios of intermolecular versus molecule-substrate coupling due to different charge-transfer and lattice-matching properties. These results have important implications for the use of TCNE as a molecular building block in contact with noble metals since the organic/inorganic interface for this molecule can vary so dramatically in terms of charge and bonding properties. This behavior might potentially be exploited to enable the controlled tuning of molecular properties for future device applications.

Acknowledgment. This work was supported in part by NSF Grants EIA-0205641 and CCR-0210176. D.W. is grateful for funding by the Alexander von Humboldt Foundation. Y.W. thanks the Miller Institute for a research fellowship. B.M.B. thanks the University of California President's Postdoctoral Fellowship Program for funding.

References

- (1) Chowdhury, S.; Kebarle, P. *J. Am. Chem. Soc.* **1986**, *108*, 5453.
- (2) Foster, R. *Organic charge-transfer complexes*; Academic Press: New York, 1969.
- (3) Masnovi, J. M.; Kochi, J. K. *J. Am. Chem. Soc.* **1985**, *107*, 6781.
- (4) Manriquez, J. M.; Yee, G. T.; McLean, R. S.; Epstein, A. J.; Miller, J. S. *Science* **1991**, *252*, 1415.
- (5) Zhang, J.; Enslin, J.; Ksenofontov, V.; Gutlich, P.; Epstein, A. J.; Miller, J. S. *Angew. Chem., Int. Ed.* **1998**, *37*, 657.
- (6) Miller, J. S. *Inorg. Chem.* **2000**, *39*, 4392.
- (7) Jain, R.; Kabir, K.; Gilroy, J. B.; Mitchell, K. A. R.; Wong, K. C.; Hicks, R. G. *Nature* **2007**, *445*, 291.
- (8) Pokhodnya, K. I.; Epstein, A. J.; Miller, J. S. *Adv. Mater.* **2000**, *12*, 410.
- (9) Haskel, D.; Islam, Z.; Lang, J.; Kmety, C.; Srajer, G.; Pokhodnya, K. I.; Epstein, A. J.; Miller, J. S. *Phys. Rev. B* **2004**, *70*, 054422.
- (10) Tengstedt, C.; de Jong, M. P.; Kanciurowska, A.; Carlegrem, E.; Fahlman, M. *Phys. Rev. Lett.* **2006**, *96*, 057209.
- (11) Long, J. R. In *Chemistry of Nanostructured Materials*; Yang, P., Ed.; World Scientific Publishing: Hong Kong, 2003; p 291.
- (12) Erley, W. *J. Phys. Chem.* **1987**, *91*, 6092.
- (13) Erley, W.; Ibach, H. *J. Phys. Chem.* **1987**, *91*, 2947.
- (14) Pan, F. M.; Hemminger, J. C.; Ushioda, S. *J. Phys. Chem.* **1985**, *89*, 862.
- (15) Chen, W.; Madhavan, V.; Jamneala, T.; Crommie, M. F. *Phys. Rev. Lett.* **1998**, *80*, 1469.
- (16) Eigler, D. M.; Schweizer, E. K. *Nature* **1990**, *344*, 524.
- (17) Bartels, L.; Meyer, G.; Rieder, K. H. *Phys. Rev. Lett.* **1997**, *79*, 697.
- (18) Sánchez-Portal, D.; Ordejón, P.; Artacho, E.; Soler, J. M. *Int. J. Quantum Chem.* **1997**, *65*, 453.
- (19) Troullier, N.; Martins, J. L. *Phys. Rev. B* **1991**, *43*, 1993.
- (20) Here we compare electron affinities for atomic and molecular elements as referenced to the neutral species (the trend would be identical if we were to use first ionization energies).
- (21) Lide, D. R. *CRC handbook of chemistry and physics*, 85th ed.; CRC Press: Boca Raton, FL, 2004.
- (22) Bélemlilga, D.; Gillet, J. M.; Becker, P. J. *Acta Crystallogr. Sect. B: Struct. Sci.* **1999**, *55*, 192.
- (23) Bekoe, D. A.; Trueblood, K. N. *Z. Kristallogr.* **1960**, *113*, 1.
- (24) Little, R. G.; Pautler, D.; Coppens, P. *Acta Crystallogr. Sect. B: Struct. Sci.* **1971**, *B 27*, 1493.
- (25) Kamna, M. M.; Graham, T. M.; Love, J. C.; Weiss, P. S. *Surf. Sci.* **1998**, *419*, 12.
- (26) Her, J. H.; Stephens, P. W.; Pokhodnya, K. I.; Bonner, M.; Miller, J. S. *Angew. Chem., Int. Ed.* **2007**, *46*, 1521.
- (27) Kaim, W.; Moscherosch, M. *Coord. Chem. Rev.* **1994**, *129*, 157.
- (28) Miller, J. S. *Angew. Chem., Int. Ed.* **2006**, *45*, 2508.
- (29) Barth, J. V. *Annu. Rev. Phys. Chem.* **2007**, *58*, 375.
- (30) Miller, J. S.; Epstein, A. J. *Angew. Chem., Int. Ed.* **1994**, *33*, 385.

NL072217Y